Journal of Materials Chemistry A

Accepted Manuscript

ROYAL SOCIETY OF CHEMISTRY

www.rsc.org/materialsA

Journal of Materials Chemistry A RSCPublishing

ARTICLE

Reversible Reduction of Li_2CO_3

Cite this: DOI: 10.1039/xoxxoooooox

Na Tian,[a] Chunxiu Hua[a,b], Zhaoxiang Wang[a*] and Liquan Chen[a]

Received ooth January 2012,
Accepted ooth January 2012

DOI: 10.1039/xoxxoooooox

www.rsc.org/

Lithium carbonate (Li_2CO_3), either as a product of the conversion reaction or as an important component of the solid-electrolyte interphase (SEI) layer on the anode of a lithium ion (Li-ion) battery, is known to be chemically inactive in both reducing and oxidizing atmospheres. No sufficient evidence was shown that Li_2CO_3 can be reduced, let alone to recognize its reduction products. Here we clarify that Li_2CO_3, as a product of conversion reaction of cobalt carbonate ($CoCO_3$) upon Li insertion, can indeed be further reduced/converted to lithium carbide (Li_2C_2) and lithium oxide (Li_2O), based on spectroscopic and transmission electron microscopic analyses. These findings will have important guidance to designing electrode (materials) with more stable cycling performances, finding ways to convert some inert compounds to useful electrode materials, and search for electrode materials with higher specific capacities, as well as in understanding the excess reversible capacity of some electrode reactions.

Introduction

Multi-electron reaction is an important strategy to realize high specific capacity for an electrode material.[1] Most of the commonly used electrode materials can only intercalated/de-intercalated less than one lithium per formula unit, [2,3] far from meeting the increasing demands of the market. Electrochemical conversion is one of the most effective reactions to reach high specific Li storage capacity because it can occur in simple MX electrode material (M for transition metals, and X for O, F, S, or polyanions) [4-7] but several electrons per formula unit of the compound can participate in the reaction. It is believed that most of the reduction products, LiX, cannot be further reduced before metallic Li is deposited.

It was recently reported that Li_2CO_3 can be electrochemically decomposed to Li_2O and CO_2 at *ca*. 4.5 V with the presence of NiO [8,9] and that the FeF_2/LiF composite can be a high-capacity cathode material between 2.0 and 4.2 V [10]. Peled *et al*. [11] pointed out that Li_2CO_3, a component of the solid electrolyte interphase (SEI) layer on the anode, can be reduced to lithium carbide (Li_2C_2) and lithium oxide (Li_2O) when copper is used as the current collector, on the basis of their X-ray photoelectron spectroscopic (XPS) characterization. However, Li_2CO_3 is often found, but Li_2C_2 is rarely detected, in the SEI layer above 0.0 V *vs*. Li^+/Li. This means that Li_2CO_3 is difficult, if not possible, to be electrochemically reduced.

Recently a series of transition metal carbonates[12-16] were reported to show reversible capacities up to 1500 mAh g^{-1}, much higher than the capacity of electrochemical conversion from metal carbonates to Li_2CO_3 and metal ($MCO_3 + 2Li^+ + 2e^- \leftrightarrow Li_2CO_3 + M$; less than 500 mAh g^{-1}). Similar results have been observed in transition metal hydroxides [17-19]. Zhou *et al*.[12], based on the obtained specific capacity of a $CoCO_3$/graphene composite, suggested that Li_2CO_3 produced during the conversion reaction of $CoCO_3$ is reduced to carbon (C^0) or other low-valence carbons under the electrochemical catalysis of the newly generated Co nanoparticles. Zhang *et al*. [13] studied polypyrrole (PPy)-coated $CoCO_3$ and attributed the excess Li-storage capacity of the composite to the formation of Li_xC_2 following *Ref* 11. However, as the PPy coating can react with fresh metallic cobalt to form a high-capacity PPy-Co coordination complex [20], the reduction of Li_2CO_3 cannot be an exclusive reason for the excess capacity. Therefore, more solid evidence is required to clarify these assumptions.

In this article, we report the electrochemical reduction of Li_2CO_3 with the presence of metallic Co nanoparticles; both are products of the conversion reaction of $CoCO_3$ in a $CoCO_3$/Li cell. By careful characterization, we recognize its reduction products to be Li_2C_2 and Li_2O. In addition, both the conversion of $CoCO_3$ and the reduction of Li_2CO_3 are found electrochemically reversible between 0.0 and 3.0 V.

Experimental

In a typical synthesis, 1 g $Co(CH_3COO)_2{\cdot}4H_2O$ (Alfa Aesar) and 2 g polyvinyl pyrrolidone (Mw = 40000, Sinopharm Chemical Reagent, SCR) were dissolved in 80 mL ethylene glycol (SCR) with continuous agitation. Later 2 g urea (SCR) was added into the solution in a 100 mL autoclave. The autoclave was then sealed with Teflon and heated at 200 °C for 24 h. The precipitate was rinsed with deionized water and ethyl alcohol in sequence and dried at 80 °C for overnight.

The electrochemical performance of $CoCO_3$ was evaluated by galvanostatic (0.1 mA cm^{-2}) cycling at room temperature. Powder electrode was prepared by mixing the powder of $CoCO_3$ (70 wt%), polyimide as binder (10 wt%) and carbon

black (20 wt%) into slurry. The slurry was cast onto a Cu foil to form the working electrode. With fresh lithium foil as the counter electrode, 1 mol L^{-1} $LiPF_6$ dissolved in a mixture of ethylene carbonate (EC) and dimethyl carbonate (DMC) (1:1 v/v) as the electrolyte, and Celgard 2300 as the separator, two-electrode ($CoCO_3$/Li) button cells were assembled in an Ar-filled glove box and cycled between 0.0 and 3.0 V *vs*. Li^+/Li. The test cells were dissembled in the glove box after galvanostatic charge/discharge treatments. The working electrode was taken out of the cell and rinsed with DMC for several times before vacuum-dried for 12 h in a mini-chamber of the glove box at room temperature. The powder material was scraped off the Cu foil for other tests.

The morphology of the as-prepared $CoCO_3$ powder was characterized on a field-emission scanning electron microscope (Hitachi S-4800). The acceleration voltage of the transmission electron microscope (TEM, Tecnai G2 F20 U-TWIN) was 200 kV. X-ray diffraction (XRD) pattern was recorded on a Bruker D8 Advance X-ray diffractometer equipped with a monochromatized Cu Kα radiation (λ = 1.5418Å). Fourier-transformed infrared (FTIR) spectra of the powder were recorded on a VERTEX 70 V spectrometer. The Raman spectra were recorded on a Renishaw Via-Reflex Raman spectrometer with a resolution of 2 cm^{-1} and laser radiation of 532 nm. In order to protect the sample from air pollution, the sample for the Raman spectrum was air-tightly sealed between two quartz plates in the glove box while the FTIR sample was analysed in the vacuum chamber of the spectrometer.

Results and discussion

The morphology of the prepared $CoCO_3$ is shown in Fig.1a. The primary $CoCO_3$ particles (*ca*. 100 nm) aggregate into leechee-like secondary particles of 1-3 μm in diameter. Such powder is expected to have a high tap density. Fig.1b shows the XRD patterns of the as-prepared $CoCO_3$. All the diffraction peaks can be indexed to rhombohedral $CoCO_3$ (JCPDS 78-0209).

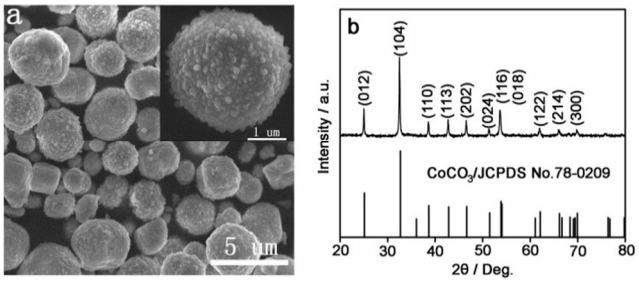

Fig. 1 SEM images (a) and XRD pattern (b) of the as-prepared $CoCO_3$

Fig.2 shows the electrochemical performances of $CoCO_3$ cycled between 0.0 V and 3.0 V *vs*. Li^+/Li. The discharge profile contains a long plateau starting at *ca*. 1.0 V in the initial discharge (Fig. 2a). This plateau becomes short and its onset potential rises to *ca*. 1.5 V in the 2nd cycle. In the subsequent cycles, it drops and finally becomes stable at 1.2 V. Except for the dropping of the starting potential of the discharge plateau, the discharge profiles of different cycles are very similar to each other. In contrast, the shape of the charge profile does not change with cycling. The reversible capacity is *ca*. 1660 mAh g^{-1} in the first cycle. Even if the capacity of the carbon black (CB) and binder PI (a total of *ca*. 300 mAh g^{-1}; inset of Fig.2a) in the electrode is considered, this value is still much higher than that of most other electrode materials that store lithium ions by way of conversion reactions. Therefore, some other reactions should have taken place in the material except for the primary conversion from $CoCO_3$ to Li_2CO_3 and metallic Co. The capacity drops in the following few cycles but is quickly stabilized at *ca*. 1500 mAh g^{-1} (Fig.2b), a behavior commonly observed in other electrode materials. Meanwhile, the coulombic efficiency of the cell quickly increases to about 100% in a few cycles. These indicate that $CoCO_3$ can be a promising high-capacity anode material for Li-ion batteries.

Raman and FTIR spectroscopy were employed to recognize the structural variation of $CoCO_3$ during the first discharge/recharge cycle (Fig.3). The selected Raman spectrum (only for the range where the characteristic peaks are located) of the $CoCO_3$ and its possible reaction products Li_2CO_3 and Li_2C_2 at various discharge/recharge potentials are shown in Fig.3a. It is clear that the characteristic peak of $CoCO_3$ (at 670 cm^{-1}) completely disappears when the cell is discharged to 0.7 V and does not reappear before the cell is recharged to 3.0 V (peak at 626 cm^{-1}). It was reported that the Raman shift of many semiconductor materials moves downwards when the grain size decreases due to size-induced phonon confinement effect and surface relaxation. [21,22] This is probably true for the current $CoCO_3$. That is, red-shifting occurs for the characteristic Raman peak of $CoCO_3$ (from 670 to 626 cm^{-1}) because its grain size becomes small after discharge and recharge. Meanwhile, Li_2CO_3 is produced when the $CoCO_3$ electrode is discharged to 0.7 V, but disappears when the electrode is further discharged to 0.0 V or is recharged to 3.0 V. A combination of the Raman spectra of $CoCO_3$ and Li_2CO_3 at various potentials above 0.7 V confirms the relationship between them: $CoCO_3$ is converted to Li_2CO_3 when the cell is discharged to 0.7 V and is regenerated when the cell is recharged to 3.0 V (*Eq*. 1).

$$CoCO_3+2Li^++2e^- \leftrightarrow Co+Li_2CO_3 \quad (1)$$

This reaction involves two electrons, corresponding to a theoretical capacity of 448 mAh g^{-1}, much lower than the observed reversible capacity (1660 mAh g^{-1}). Even if the contribution of the carbon black (conductive additive) and the binder polyimide (*ca*. 300 mAh g^{-1}×0.3=90 mAh per gram of electrode ($CoCO_3$ + PI + CB); inset of Fig.2a) is considered, the origin for a net capacity of about 1120 (1660-90-448)=1120 mAh g^{-1}) remains unknown. Therefore, other reactions have to be considered in order to understand the excess capacity.

Journal of Materials Chemistry A

ARTICLE

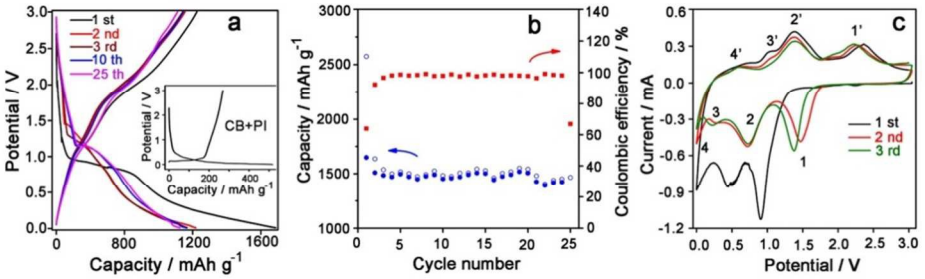

Fig. 2 Potential profile (a) and cycling performance (b) of a $CoCO_3$/Li cell between 0.0 and 3.0 V at a current density of 0.1 mA cm^{-2}. The potential profile of a cell with the conductive additive and the binder (2:1 w/w) as the working electrode in the same potential range and at the same current density is shown as inset of (a) for reference. *c* is the cyclic voltammetry of a $CoCO_3$/Li cell in the first 3 cycles at a scan rate of 0.5 mV s^{-1}

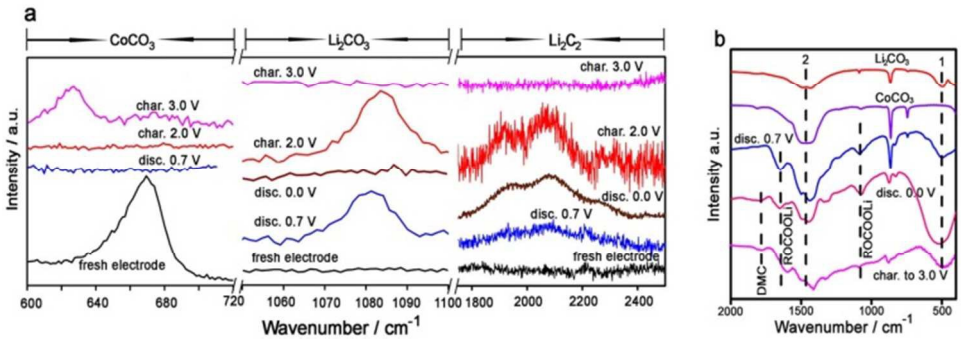

Fig. 3 Selected Raman (a) and FTIR (b) spectra of the $CoCO_3$ electrode discharged/recharged to various potentials. The FTIR spectra of commercial Li_2CO_3 and as-prepared $CoCO_3$ are shown in (b) for reference

Zhou *et al.*[12] recognized Li_2O, metallic Co and Li_2CO_3 in the discharge (0.0 V) products of $CoCO_3$ by selected area electron diffraction (SAED) and suggested the presence of species containing C=C groups according to the binding energy of C_{1s} of the discharge products by XPS, involving a total of 6 electrons in the conversion reaction. Zhang *et al.* [13], following the suggestion of Peled *et al.* [11], attributed the excess capacity of their PPy-coated $CoCO_3$ to the formation of Li_2C_2 though they did not observe any traces of Li_2C_2. Therefore, actually neither of these groups of authors observed any Li_2C_2 in discharged $CoCO_3$. By spectroscopic method, we clarify the presence of Li_2C_2 in deeply discharged $CoCO_3$.

When the cell is further discharged from 0.7 V to 0.0 V, the Raman peak of Li_2CO_3 disappears and two broad Raman peaks appear at *ca*. 1940 cm^{-1} and 2060 cm^{-1} (Fig.3a). Nylén *et al.* [23] reported that the C≡C stretching of Li_2C_2 is at 1872 cm^{-1} in the Raman spectrum. We confirmed this with the Raman spectrum of our home-prepared Li_2C_2 (Fig. S1; the preparation of Li_2C_2 was reported in *Ref*.24). Therefore, the broad band at 1940 cm^{-1} is assigned to Li_2C_2. The band at 2060 cm^{-1} is tentatively assigned to acetylene (C_2H_2) as a decomposition product of Li_2C_2 that was air-tightly sandwiched between two quartz plates under continuous laser irradiation during Raman spectroscopic analysis. These two peaks become very weak when the cell is recharged to 2.0 V. Considering the re-appearance of the characteristic Raman peak of Li_2CO_3 at 2.0 V, these actually mean the decomposition of Li_2CO_3 and the formation of Li_2C_2 below 0.7 V and that Li_2C_2 is oxidized to Li_2CO_3 when the cell is charged to 2.0 V. This is consistent with the features of the potential profiles (the similarity of the discharge profiles of different cycles).

The above decomposition and re-formation of $CoCO_3$, Li_2CO_3 and Li_2C_2 can be seen more clearly with Fourier-transformed infrared (FTIR) spectroscopy. Fig.3b shows the evolution of FTIR spectrum of the $CoCO_3$ electrode at various discharge/charge potentials. The FTIR spectra of pure $CoCO_3$, Li_2CO_3, Li_2O and Li_2C_2 are shown in Fig.S2 for reference (the electrochemical performances of Li_2C_2 will be reported elsewhere). When the cell is discharged to 0.7 V, the plateau peak at 1466 cm^{-1} (for $CoCO_3$) is divided into peaks at 1436 and 1498 cm^{-1}. Meanwhile, a strong peak appears at *ca*. 500 cm^{-1}, demonstrating the presence of Li_2CO_3. These spectral features illustrate that $CoCO_3$ is converted to Li_2CO_3 when the cell is discharged to 0.7 V. As the cell is further discharged to 0.0 V, the peak at 500 cm^{-1} becomes the dominating one in the spectrum, much stronger than the double peak around 1466 cm^{-1} for residual Li_2CO_3. Considering that the absorption peaks of both Li_2C_2 and Li_2O are below 800 cm^{-1} (Fig.S2) and that the characteristic peaks of Li_2CO_3 at 864, 1436 and 1498 cm^{-1} are rather weak, we attribute the strong 500 cm^{-1} peak to a

combination of Li_2O and Li_2C_2 as well as some residual Li_2CO_3. Therefore, the FTIR spectral features mean the decomposition of Li_2CO_3 and the formation of Li_2O and Li_2C_2. When the cell is recharged to 3.0 V, the peak around 500 cm^{-1} becomes very weak. These results indicate the absence of Li_2O (and the re-formation of $CoCO_3$ if the Raman spectral features at 3.0 V are considered).

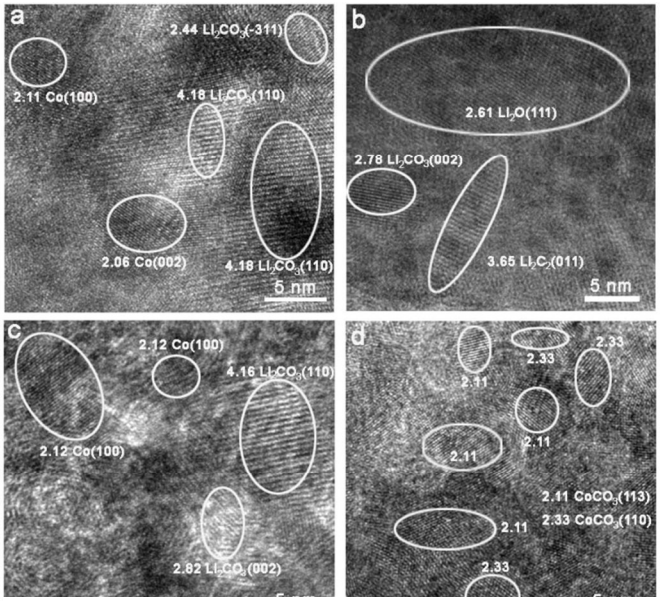

Fig. 4 HRTEM images of the $CoCO_3$ electrode at various discharge/charge states: discharged to 0.7 V (a), discharged to 0.0 V (b), recharged to 2.0 V (c), and recharged to 3.0 V (d)

The above suggestion is further supported with high-resolution transmission electron microscopic imaging (HRTEM; Fig.4). When the cell is discharged to 0.7 V, domains of Li_2CO_3 (~10 nm) and Co (~5 nm) clusters are clearly seen (Fig.4a). This means that $CoCO_3$ is decomposed to Li_2CO_3 and metallic Co at 0.7 V in the primary conversion reaction. When the cell is further discharged to 0.0 V, domains of Li_2O (~15 nm), Li_2C_2 (~10 nm) as well as Li_2CO_3 (~5 nm) come into being (Fig.4b). These illustrate that Li_2CO_3 is decomposed to Li_2O and Li_2C_2 upon deep discharge. No $CoCO_3$ can be found in the view field below 0.7 V. When the cell is recharged to 2.0 V, Li_2CO_3 and metallic Co can be observed (Fig.4c). When the cell is finally recharged to 3.0 V, small particles (<5 nm) can be observed (Fig.4d), implying the low crystallinity of the regenerated $CoCO_3$. This makes sense and explains the red-shifting of the Raman peak from 670 cm^{-1} in the as-prepared $CoCO_3$ to 626 cm^{-1}. The corresponding Fast Fourier Transform (FFT) of the above HRTEM images (Fig.S3) and some other important images (Fig.S4) are also supplied in the supporting information.

The above results show that Li_2CO_3 can be reversibly reduced to Li_2C_2 and Li_2O thanks to the presence (electrochemical catalysis effect) of the freshly generated metallic Co nanoparticles, corresponding to a theoretical capacity of 1122 mAh g^{-1}). Based on these, the electrochemical reduction of Li_2CO_3 in this work can be written as

$$Li_2CO_3+5Li^+ +5e^- \leftrightarrow 0.5Li_2C_2 + 3Li_2O \quad (2)$$

With these understandings, the CV profile of the $CoCO_3$ electrode (Fig.2c) can be better explained. The redox peak couples (1/1′) and (2/2′) are attributed to the electrochemical conversion reaction (*Eq*.1), and reduction/oxidation (*Eq*.2) respectively. These two reactions involve a total theoretical capacity of 1570 mAh g^{-1} or 7 electrons per formula unit of $CoCO_3$. We attribute the 3rd redox peak couple (3/3′) in Fig.2c to the decomposition of some other SEI components. However, it is difficult to determine the reactants, the products or the contribution of each to the total capacity in the present work. Finally the 4th redox peak couple (4/4′) is assigned to the Li-ion insertion/extraction in the carbon black and the binder additives, corresponding to a capacity of *ca*. 90 mAh per gram of electrode.

The fact that Li_2CO_3 can be reduced to Li_2C_2 and Li_2O makes $CoCO_3$ and other metal carbonates promising high-capacity anode materials for Li-ion batteries. However, the significance of the findings here is not stopped at that. In this work, the valence of the carbon decreases from C^{4+} to C^-, involving a total of 5 electrons. Therefore, the reduction of Li_2CO_3 is a typical multi-electron reaction, by which a very high specific capacity can be obtained in such a simple compound. The reduction of Li_2CO_3 also has its significance in electrode investigation and designing. On one hand, as nanosized Li_2CO_3 is a very common component of the SEI layer on the anode for Li-ion batteries using carbonate-based nonaqueous electrolytes, the stability of the SEI layer should be carefully considered on designing the anode, especially when there are metal nanoparticles, electrochemically reduced (by electrochemical conversion of Fe_2O_3, for example) or intentionally (as conductive or protective additives) or unintentionally (as impurities during material processing and electrode fabrication) added, in the anode discharged to low potentials. The presence and the catalysis effect of the metal nanoparticles might damage the SEI layer and the cycling stability of the cell as well as the possible growth of metal dendrites. On the other hand, there have been many reports in recent years that the obtained capacity of transition metal containing compounds such as cobalt oxides [25], iron oxides [26, 27], copper fluoride [28] and ruthenium oxides [29] overpasses their theoretical capacities. Most authors simply attribute these phenomena to some synergistic effect between the transportation and interaction of the electrons and the lithium ions, but some authors ascribe them to the transition metal catalyzed decomposition of the SEI layer components. Our findings illustrate the possibility of some SEI components and their contribution to the total capacity. Therefore, the stability of Li_2CO_3 and the impact of its reduction on the coulombic efficiency and the cycling performance of the cell should be re-evaluated when the transition metal compound can be reduced to metals.

Conclusions

In summary, reversible electrochemical reduction of Li_2CO_3 is experimentally confirmed with the presence of freshly

generated Co nanoparticles. For the first time, we structurally clarify its reduction products to be Li_2C_2 and Li_2O. Involving 5 electrons per formula unit, this reduction makes the traditionally believed inactive Li_2CO_3 a novel and attractive high-capacity electrode material for lithium storage between 0.0 and 3.0 V *vs*. Li^+/Li. The observation that Li_2CO_3 can be electrochemically reduced makes $CoCO_3$ and other (transition) metal carbonates promising high-capacity anode materials for lithium ion batteries. More significance of these findings lies in their guidance to electrode designing and the prediction or explanation of the performance of some transition metal electrodes with very high reversible capacities. That is, on designing an electrode that contains transition metal nanoparticles or where such nanoparticles can be reduction products of the electrode reaction, the possibility of the decomposition of some components of the SEI layer should be evaluated. Such decomposition might lead to degradation of the SEI layer and the electrode performance. On the other hand, the origin for the excess capacity of some transition metal compounds that store lithium by way of electrochemical conversion should be re-considered. Decomposition of some components and their re-formation, take Li_2CO_3 for example, of the SEI layer in carbonate-based electrolytes can probably contribute extra reversible capacity to the electrode.

Acknowledgement

This work was financially supported by the National 973 Program of China (No.2015CB251100) and the National Natural Science Foundation of China (NSFC, No. 11234013).

Notes and references

[a]*Key Laboratory for Renewable Energy, Chinese Academy of Sciences, Beijing Key Laboratory for New Energy Materials and Devices, Beijing National Laboratory for Condensed Matter Physics, Institute of Physics, Chinese Academy of Sciences, P. O. Box 603, Beijing 100190, China. Tel.& Fax: +86-10-82649050; E-mail: zxwang@iphy.ac.cn.*
[b]*Research Institute, Ningde Amperex Technology Limited, Fujian 352100, China*

1. X. P. Gao and H. X. Yang, *Energy Environ. Sci.*, 2010, **3**, 174-189.
2. J. R. Dahn, T. Zheng, Y. H. Liu and J. S. Xue, *Sci.*, 1995, **270**, 590-593.
3. H. Moriwake, A. Kuwabara, C. A. J. Fisher, R. Huang, T. Hitosugi, Y. H. Ikuhara, H.Oki and Y. Ikuhara, *Adv. Mater.*, 2013, **25**, 618-622.
4. A. L. M. Reddy, M. M. Shaijumon, S. R. Gowda and P. M. Ajayan, *Int. Nano Lett.*, 2009, **9**, 1002-1006.
5. T. Stephenson, Z. Li, B. Olsenab and D. Mitlin. *Energy Environ. Sci.,* 2014, **7**, 209-231.
6. Y. Ma and S. H. Garofalini, *J. Am. Chem. Soc.*, 2012, **134**, 8205-8211.
7. C. X. Zu and H. Li, *Energy Environ. Sci.,* 2011, **4**, 2614-2624.
8. Y. L. Liu, R. Wang , Y. C. Lyu, H. Li and L.Q. Chen, *Energy Environ. Sci.,* 2014, **7**, 677-681.
9. C. Ling, R. G. Zhang, K. Takechi and F. Mizuno, *J. Phys. Chem. C*, 2014, **118**, 26591-26598.
10. S. W. Kim, K. W. Nam, D.H. Seo, J. Hong, H. Kim, H. Gwon and K. Kang, *Nano Today*, 2012, **7**, 168-173.
11. V. Eshkenazi, E. Peled, L. Burstein and D. Golodnitsky, *Solid State Ionics*, 2004, **170**, 83-91.
12. L.W. Su *et al*. *Nano Energy,* 2013, *2*, 276-282.
13. Z. J. Ding, B. Yao, J. K. Feng and J. X. Zhang, *J. Mater. Chem. A*, 2013, **1**, 11200-11209.
14. G. Y. Huang, S. M. Xu, Y. Yang, H. Y. Sun, Z. B. Li, Q. Chen and S. S. Lu, *Mater. Lett.*, 2014, **131**, 236-239.
15. Y. R. Zhong, L.W. Su, M. Yang, J. P. Wei and Z. Zhou, *ACS Appl. Mater. Interfaces*, 2013, **5**, 11212-11217.
16. L. K. Zhou, X. H. Kong, M. Gao, F. Lian, B. J. Li, Z. F. Zhou, H. Q. Cao, *Inorg. Chem.*, 2014, **53**, 9228-9234.
17. Y. S. He, D. W. Bai, X. W. Yang, J. Chen, X. Z. Liao and Z. F. Ma, *Electrochem. Commun*., 2010, **12**, 570-573.
18. G. Chen, E. G. Fu, M. Zhou, Y. Xu, L. Fei, S. G. Deng, V. Chaitanya, Y. Q. Wang and H. M. Luo, *J. Alloys Compd.*, 2013, **578**, 349-354.
19. J. J. Ma, T. Yuan., Y. S. He, J. L. Wang, W. M. Zhang, D. Z. Yang, X. Z. Liao and Z. F. Ma, *J. Mater. Chem. A*, 2014, 1-7.
20. B. K. Guo, Q. Y. Kong, Y. Zhu, Y. Mao, Z. X. Wang, M. X. Wan, and L. Q. Chen, *Chem. Eur. J.*, 2011, **17**, 14878-14884.
21. W. J. Duan, S. H. Lu, Z. L. Wu and Y. S. Wang, *J. Phys. Chem. C*, 2012, **116**, 26043-26051.
22. C. C. Yang and S. Li, *J. Phys. Chem. C. B*, 2008, **112**, 14193 -14197.
23. J. Nylén, S. Konar, P. Lazor, D. Benson and U. Häussermann, *J. Chem. Phys*., 2012, **137**, 224507.
24. J. T. He, X. Y. Song, W. W. Xu, Y. Y. Zhou, M. Seyring and M. Rettenmayr, *Mater. Lett.*, 2013, **94**, 176-178.
25. X. Guan, J. W. Nai, Y. P. Zhang, P. X. Wang, J. Yang, L. R. Zheng, J. Zhang, L.Guo, *Chem. Mater.,* 2014, *26*, 5958-5964.
26. L. W. Su, Y. R. Zhong and Z. Zhou, *J. Mater. Chem. A*, 2013, **1**, 15158-15166.
27. Y. Z. Jiang, D. Zhang, Y. Li, T. Z. Yuan, N. Bahlawane, C. Liang, W. P. Sun, Y. H. Lu and M. Yan, *Nano Energy*, 2014, **4**, 23-30.
28. Y. F. Zhukovskii, P. Balaya , M. Dolle, E.A. Kotomin and J. Maier, *Phys. Rev. B*, 2007, **76**, 235414.
29. Y. Y. Hu, Z. G. Liu, K. Nam, O. J. Borkiewicz, J. Cheng, X. Hua, M. T. Dunstan, X. Q. Yu, K. M.Wiaderek, L.S. Du, K. W. Chapman, P. J. Chupas, X. Q. Yang and C. P. Grey. *Nat. Mater.*, 2013, **12**, 1130-1136.

Graphical Abstract

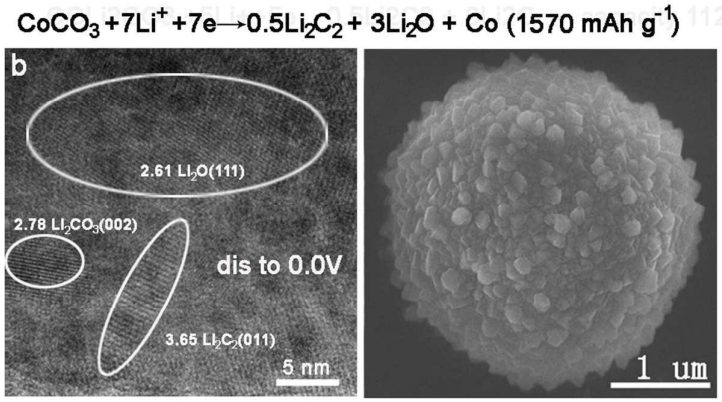

HRTEM images of the $CoCO_3$ electrode discharged to 0.0 V and SEM image